RiESTech
Recent in Engineering Science and Technology

MBI

Article

Analysis of the Effect of Air Inlet Filter Replacement on Gas Turbine Performance at Unit 1A of Bekasi Power Combined Cycle Power Plant

Gilang Fitra Ardiansyah [1], Arifia Ekayuliana [2,*]

[1] Bachelor of Applied Energy Generation Engineering Technology Program, Department of Mechanical Engineering, Politeknik Negeri Jakarta, Depok 16424, Indonesia,
[2] Department of Mechanical Engineering, Politeknik Negeri Jakarta, Depok 16424, Indonesia
* Correspondence: arifia.ekayuliana@mesin.pnj.ac.id

Abstract: Air inlet filters protect gas turbine compressors from fouling, yet quantitative evidence of how filter replacement changes the performance of an operating unit remains limited. This study evaluates the effect of air inlet filter replacement on the GT1A gas turbine at Unit 1A of Bekasi Power Combined Cycle Power Plant. Secondary data from the control system and operator check sheets were compared before (11 November 2025) and after (7 January 2026) replacement, using snapshots at 00:00, 12:00 and 16:00. Compressor, combustion-chamber, turbine and thermal efficiencies were calculated from Brayton-cycle relations, and the sensitivity to hot-gas properties was tested. Filter differential pressure fell from 76–82 to 45–46 mmH_2O. Compressor efficiency rose from 78.85 – 81.76% to 88.71–90.88%, and thermal efficiency from 18.23–21.58% to 27.92–30.82%, while generator load increased from 37.4 to 38.5–38.9 MW. A fishbone (6M) analysis supported by failure mode and effect analysis identified environmental factors, mainly airborne dust, as the dominant cause of filter replacement. The improvement coincides with filter replacement and a compressor wash performed in the same period, so the effect of the filter alone cannot be separated.

Keywords: Engine fault detection; Marine diesel engine; Physical consistency; Monotonic constraints; Explainable boosting machine; SHAP; Label convention; Positive control

Citation: Ardiansyah, G. F., Ekayulianan, A. (2026). Analysis of the Effect of Air Inlet Filter Replacement on Gas Turbine Performance at Unit 1A of Bekasi Power Combined Cycle Power Plant. Recent in Engineering Science and Technology, 4(4), 245–254. Retrieved from https://www.mbi-jounals.com/index.php/riestech/article/view/175.

Academic Editor: Yudhi Ariadi

Received: 22 July 2026
Accepted: 19 October 2026
Published: 31 October 2026

Publisher's Note: MBI stays neutral with regard to jurisdictional claims in published maps and institutional affiliations.

Copyright: © 2026 by the authors. Licensee MBI, Jakarta, Indonesia. This article is an open access article distributed under MBI license (https://mbi-journals.com/licenses/by/4.0/).

1. Introduction

Gas turbines are widely used in simple-cycle and combined-cycle plants because of their fast start-up and operational flexibility. The air drawn from the atmosphere passes through an inlet filter house before it enters the compressor, so the condition of the filter governs the pressure, cleanliness and mass flow of the air supplied to the whole cycle [1,2]. Particles that penetrate the filter cause fouling, erosion and corrosion of the compressor blades, which lowers airflow, pressure ratio and compressor efficiency and, in turn, reduces power output and thermal efficiency [3–5]. At the same time, dust loading raises the pressure drop across the filter house, which acts as an inlet pressure loss [2,6].

Earlier studies have addressed parts of this problem. Simanjuntak et al. [7] compared the compressor of a gas turbine before and after air inlet filter replacement at a power plant in Batam, Indonesia, and reported compressor efficiency gains of about 2 and 3 percentage points at 38 and 39 MW. Purwanto [8] analysed how the compressor inlet temperature affects compressor, combustion-chamber and thermal efficiency of a gas turbine at the Grati power plant. Effiom et al. [9] investigated inlet air filtration for offshore gas turbines experimentally, and Jin et al. [6] proposed a model-based approach to diagnose filter condition in gas turbine air intake systems. Köse and Yılmazoğlu [10] examined the effect of inlet-filter blockage within a study of periodic gas turbine maintenance and determined a cost-optimal filter replacement period. Kurz and Brun [3] and Meher-Homji and Bromley [4] reviewed degradation and fouling mechanisms in

general. These works concentrate on a single performance indicator, on ambient-temperature effects, or on laboratory and model-based diagnosis.

To the authors' knowledge, field evidence that links the measured filter differential pressure with the compressor, combustion-chamber, turbine and thermal efficiencies of one operating industrial unit before and after a filter replacement, together with a structured analysis of why the replacement was needed, is still limited. The present study addresses this gap for the GT1A gas turbine at Unit 1A of Bekasi Power Combined Cycle Power Plant. Control-system and check-sheet data from before and after replacement are used to recompute the four efficiencies from Brayton-cycle relations, including a sensitivity check on hot-gas properties, and fishbone (6M) and failure mode and effect analysis (FMEA) are applied to identify the causes of filter deterioration [11–13]. The results show a clear improvement of all efficiencies after replacement, but also that the filter pressure loss alone cannot explain its full size, which is discussed in Section 3.

2. Materials and Experiment Methods

2.1. Research Object

The object is the GT1A gas turbine and its air inlet filter system at Unit 1A of Bekasi Power Combined Cycle Power Plant (Cikarang, West Java, Indonesia). The unit is a General Electric PG6581B gas turbine generator with a nominal output of 37.97 MW, fired with natural gas and monitored by a Mark VI control system (DCS). The filter elements were installed on 1 November 2022 and replaced on 19 November 2025.

2.2. Data and Sampling

The study is quantitative and comparative and uses secondary data from the DCS and the operators' two-hourly check sheets. Purposive sampling was applied to select days with relatively stable operation: 11 November 2025 (before replacement, eight days before the physical replacement) and 7 January 2026 (after replacement). On each day three snapshots were taken: night (00:00), afternoon (12:00) and evening (16:00). Each value is a single observation logged at the stated hour (n = 1 per snapshot), not an average. The inputs are compressor inlet temperature (T_1) and pressure (P_1), compressor discharge temperature (T_2) and pressure (P_2), turbine inlet temperature (T_3), exhaust temperature (T_4), fuel gas flow ($\dot{m}_f$), generator load, and the differential pressure of the filter house (ΔP_f, "DP Inlet Filter" on the check sheet, in mmH_2O; 1 mmH_2O = 9.80665 Pa). Pressures are absolute (kPa A) as logged by the control system. All inputs are listed in Table 1.

2.3. Assumptions

The analysis assumes steady operation at each snapshot, ideal-gas behaviour, no pressure loss in the combustor, and expansion of the hot gas from P_2 to P_1 (exhaust at compressor inlet pressure). Because the real expansion ratio is lower (combustor and exhaust-duct losses), the ideal expansion work is overestimated and the calculated turbine efficiency is a conservative, lower estimate. T_3 is the combustion-chamber temperature measured and logged by the DCS. In the base case, air properties are used throughout (γ_a = 1.4), following the original calculation. Because this overestimates γ on the hot side, a sensitivity case uses γ_g = 4/3, $c_{p,g}$ = 1.148 kJ kg^{-1} K^{-1} for combustion products and $c_{p,a}$ = 1.005 kJ kg^{-1} K^{-1} for air [1].

2.4. Performance Calculation

2.4.1. Compressor and Combustion Chamber

The isentropic compressor outlet temperature and the compressor efficiency are [14,15]:

$$T_{2s} = T_1 \left(\frac{P_2}{P_1}\right)^{\frac{\gamma_a - 1}{\gamma_a}} \quad (1)$$

$$\eta_c = \frac{T_{2s} - T_1}{T_2 - T_1} \quad (2)$$

The combustion-chamber efficiency is defined, as in the original calculation, as a temperature-based index comparing the actual temperature rise with the rise that would follow from isentropic compression:

$$\eta_{cc} = \frac{T_3 - T_2}{T_3 - T_{2s}} \quad (3)$$

2.4.2. Turbine

$$T_{4s} = T_3 \left(\frac{P_1}{P_2}\right)^{\frac{\gamma_g - 1}{\gamma_g}} \quad (4)$$

$$\eta_t = \frac{T_3 - T_4}{T_3 - T_{4s}} \quad (5)$$

In the base case $\gamma_g = \gamma_a = 1.4$.

2.4.3. Thermal Efficiency and Mass Flows

Three mass flows are distinguished: the air mass flow $\dot{m}_a$ through the compressor, the fuel mass flow $\dot{m}_f$ (natural gas, from the DCS), and the gas mass flow through the turbine $\dot{m}_g$, with $\dot{m}_g = \dot{m}_a + \dot{m}_f$ (Equation (6)). The air mass flow is not recorded at this unit; the fuel flow is about 2% of the exhaust flow in the manufacturer's data, so $\dot{m}_g \approx \dot{m}_a$. Only efficiencies, which are ratios in which the mass flow cancels, are reported; absolute powers are therefore not computed from $\dot{m}_f$.

$$\dot{m}_g = \dot{m}_a + \dot{m}_f \quad (6)$$

$$W_c = \dot{m}_a c_{p,a}(T_2 - T_1), \quad W_t = \dot{m}_g c_{p,g}(T_3 - T_4) \quad (7)$$

$$Q_{in} = \dot{m}_g c_{p,g} T_3 - \dot{m}_a c_{p,a} T_2 \quad (8)$$

$$\eta_{th} = \frac{W_t - W_c}{Q_{in}} \quad (9)$$

In the base case (constant properties, $\dot{m}_g = \dot{m}_a$) Equation (9) reduces to

$$\eta_{th} = \frac{(T_3 - T_4) - (T_2 - T_1)}{T_3 - T_2} \quad (10)$$

This cycle efficiency is a temperature-based indicator for comparing operating conditions; it is not the fuel-based electrical efficiency of the plant.

2.5. Filter Service Life

The service life is $T = t_2 - t_1$ (Equation (11)), with t_1 the installation date and t_2 the replacement date, and the total operating hours are $H = T \times H_o$ (Equation (12)), with H_o = 4,032 h per year the annual operating hours from plant records.

$$T = t_2 - t_1, \quad H = T \times H_o \quad (11, 12)$$

2.6. Fishbone and FMEA Analysis

Causes of filter deterioration were collected by field observation and interviews with five operation and maintenance respondents and grouped into the six categories Man,

Method, Machine, Material, Measurement and Environment [11,12]. For FMEA, severity (S), occurrence (O) and detection (D) were scored from 1 to 10 for the dominant failure mode of each category, and the risk priority number was calculated as [13]:

$$RPN = S \times O \times D \tag{13}$$

3. Results and Discussion

3.1. Operating Data and Filter Pressure Drop

Table 1 lists the inputs of all six snapshots. The differential pressure across the filter house was 76–82 mmH_2O (745–804 Pa) before and 45–46 mmH_2O (441–451 Pa) after replacement, a reduction of 294–363 Pa, or about 0.3 kPa. Relative to an ambient pressure of about 101 kPa, the inlet pressure loss therefore decreased by only about 0.3%. The compressor inlet pressure logged by the control system (103.5–110.0 kPa) does not resolve a change of this size: the January values are lower, not higher, than the November values, and all values exceed the standard atmospheric pressure of 101.3 kPa, which suggests a transmitter offset that could not be verified. It was used only as the recorded input of the pressure ratio.

Table 1. Measured inputs of GT1A before (11 November 2025) and after (7 January 2026) filter replacement.

Parameter	Unit	11 November 2025 (before)			7 January 2026 (after)		
		00:00	12:00	16:00	00:00	12:00	16:00
Generator load	MW	37.42	37.40	37.40	38.85	38.50	38.65
T_1	K	301.05	304.35	303.65	299.95	305.25	305.05
P_1 (abs.)	kPa	108.5	110.0	109.7	103.5	109.2	108.0
T_2	K	633.65	646.05	645.05	625.95	636.75	635.25
P_2 (abs.)	kPa	1032	1012	1015	1146	1158	1153
T_3	K	1338.15	1323.15	1326.15	1378.15	1355.15	1358.15
T_4	K	853.55	858.00	857.15	820.34	823.05	822.15
$\dot{m}_f$ (fuel gas)	kg/s	2.74	2.80	2.78	2.36	2.49	2.45
Filter ΔP_f [1]	mmH_2O	82	76	76	45	46	46
P_2/P_1	–	9.51	9.20	9.25	11.07	10.60	10.68

[1] Read from the operators' check sheet ("DP Inlet Filter"); values transcribed from the original handwritten log.

Ambient conditions were comparable: T_1 differed by −1.1 to +1.4 K between the two days at the same hour. Generator load was 1.1–1.4 MW (3–4%) higher after replacement. The compressor discharge pressure rose from 1012–1032 to 1146–1158 kPa, so that the pressure ratio increased from 9.20–9.51 to 10.60–11.07, while the compressor discharge temperature was 7.7–9.8 K lower, the exhaust temperature 33–35 K lower and T_3 32–40 K higher. Fuel gas flow fell from 2.74–2.80 to 2.36–2.49 kg/s.

Physically, the filter house is a pressure loss in series with the compressor. For a single-shaft machine at constant speed the compressor swallows an almost fixed volume flow, so the air mass flow scales with the inlet density, i.e. with P_1/T_1, and the discharge pressure scales with P_1 for a given pressure ratio [1]. A 0.3 kPa smaller inlet loss therefore raises air mass flow and P_2 by roughly 0.3% only. The measured rises in discharge pressure (11–14%) and pressure ratio (15–16%) are far larger. A heavily loaded filter also lets more fine particles reach the compressor, where deposits reduce flow capacity and efficiency [3,4]; such deposits are not removed by the filter change itself, although a new filter limits further fouling. Consequently, the changes in Table 1 cannot be attributed to the lower filter pressure loss alone. A compressor wash was carried out in the period between the two datasets during the maintenance window around 19 November 2025. Because fouling deposits are removed by washing and not by changing the filter [4], the

wash most likely accounts for a large part of the recovery of compressor efficiency, and the effect of the filter replacement cannot be separated from it. Differences in inlet guide vane position or firing-temperature control and instrument calibration may also have contributed. Filter condition itself is characterised by the relation between flow resistance and dust loading described in ISO 29461-1 [16].

3.2. Compressor Efficiency

Table 2 summarises the four calculated efficiencies and Figure 1 compares them for matching times of day.

Table 2. Calculated efficiencies of GT1A (base case, $\gamma = 1.4$).

Snapshot	Load (MW)	η_c (%)	η_{cc} (%)	η_t (%)	η_{th} (%)
11 Nov 2025, 00:00	37.42	81.76	92.07	76.31	21.58
11 Nov 2025, 12:00	37.40	78.85	90.36	74.87	18.23
11 Nov 2025, 16:00	37.40	79.01	90.48	75.18	18.73
7 Jan 2026, 00:00	38.85	90.88	96.20	81.45	30.82
7 Jan 2026, 12:00	38.50	88.71	95.05	80.02	27.92
7 Jan 2026, 16:00	38.65	89.35	95.36	80.27	28.47

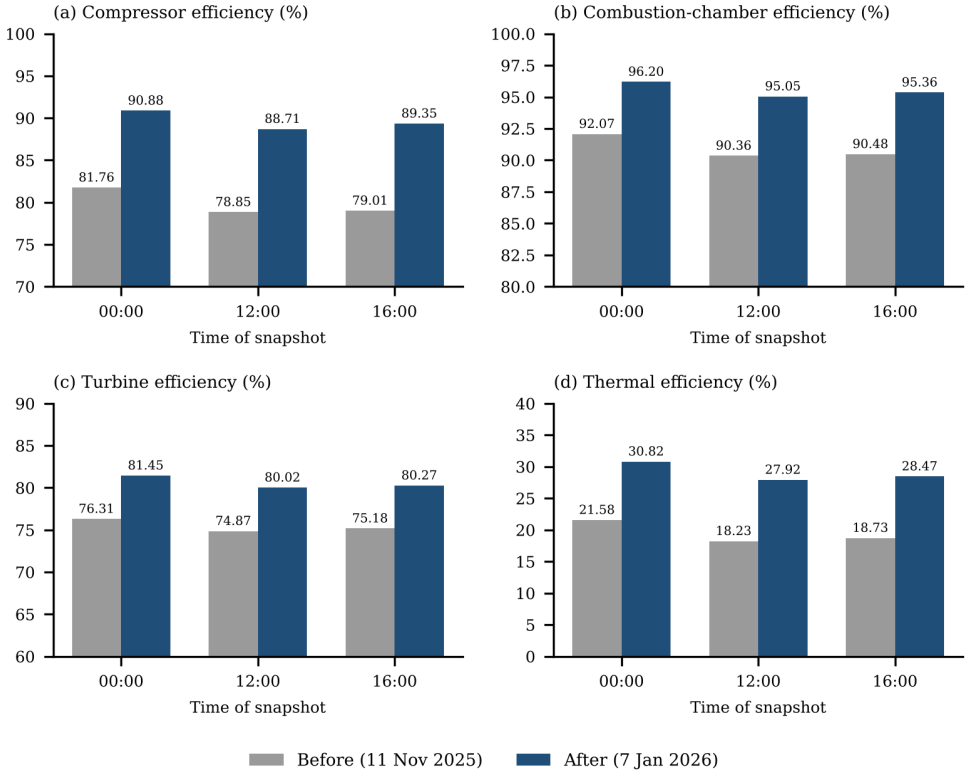


Figure 1. Efficiencies of GT1A before and after air inlet filter replacement: (a) compressor, (b) combustion chamber, (c) turbine and (d) thermal efficiency.

Compressor efficiency rose from 78.85–81.76% to 88.71–90.88%, an increase of 9.1–10.3 percentage points at matching times (Table 2, Figure 1a). Equation (2) shows the origin: after replacement the pressure ratio is 15–16% higher, so the ideal temperature rise $T_{2s} - T_1$ grows by 24–25 K, whereas the actual rise $T_2 - T_1$ shrinks by 7–11 K. A higher pressure ratio reached with a smaller temperature rise is the signature of a less degraded compressor, since fouling lowers airflow, pressure ratio and efficiency [4]. Simanjuntak et

al. [7] found gains of about 2 and 3 percentage points at 38 and 39 MW after filter replacement; the gain here is three to five times larger, which is consistent with the additional effect of the compressor wash. Isentropic compressor efficiencies of the order of 0.85–0.90 are usual for axial machines [1], so the post-replacement values are plausible and the pre-replacement values indicate degraded compression. Ambient temperature cannot explain the change: Purwanto [8] reported a drop of only 0.09 percentage points (92.46% to 92.37%) for a 7.4 K higher inlet temperature, whereas T_1 differed here by at most 1.4 K.

3.3. Combustion-Chamber and Turbine Efficiency

Combustion-chamber efficiency increased from 90.36–92.07% to 95.05–96.20% and turbine efficiency from 74.87–76.31% to 80.02–81.45% (Table 2, Figure 1b,c). Equation (3) is a temperature-based index: it rises when compression is more efficient even if the combustor itself is unchanged, so it shows how the compressor improvement propagates through the cycle and is not a measure of combustion completeness. For the turbine, the actual temperature drop $T_3 - T_4$ increased by 14–15%, while the ideal drop increased by only 7–8%, because the higher T_3 and expansion ratio enlarge both, but the exhaust temperature fell.

Table 3 tests the sensitivity to the property assumption of Section 2.3. With hot-gas properties the isentropic exhaust temperature is higher, the ideal drop smaller, and the turbine efficiency 7.7–8.1 percentage points higher than in the base case; the thermal efficiency is 2.0–3.7 points higher. The absolute levels therefore depend on the assumption (the base-case turbine efficiency is probably underestimated), but the change between the two datasets is robust: about +5.4 points for the turbine and +8.1 to +8.5 points for the thermal efficiency, against +5.1 to +5.2 and +9.2 to +9.7 points in the base case.

Table 3. Sensitivity of turbine and thermal efficiency to gas properties.

Snapshot	η_t base (%)	η_t hot gas (%)	η_{th} base (%)	η_{th} hot gas (%)
11 Nov 2025, 00:00	76.31	84.11	21.58	24.69
11 Nov 2025, 12:00	74.87	82.56	18.23	21.91
11 Nov 2025, 16:00	75.18	82.90	18.73	22.34
7 Jan 2026, 00:00	81.45	89.59	30.82	32.81
7 Jan 2026, 12:00	80.02	88.07	27.92	30.32
7 Jan 2026, 16:00	80.27	88.33	28.47	30.79

Base: $\gamma = 1.4$ throughout. Hot gas: $\gamma_g = 4/3$, $c_{p,g} = 1.148$ and $c_{p,a} = 1.005$ kJ kg^{-1} K^{-1} (Equations (4) and (7)–(9)).

3.4. Thermal Efficiency

The thermal efficiency indicator rose from 18.23–21.58% to 27.92–30.82% (Figure 1d), an increase of 9.2–9.7 points in the base case and 8.1–8.5 points with hot-gas properties (21.91–24.69% to 30.32–32.81%). Both levels are below the value implied by the manufacturer's nominal heat rate of 11,400 kJ/kWh (3600/11,400 = 31.6%), because the indicator neglects mechanical and generator losses and depends on T_3, which is not an independent measurement; it should be used to compare conditions, not as an absolute efficiency. The direction agrees with the finding that a growing inlet pressure loss from filter degradation reduces power and thermal efficiency [6]. Load also differs between the datasets (+1.1 to +1.4 MW). A study of a combined cycle plant reported a rise of gas turbine cycle efficiency from 31.28% at 23 MW to 45.56% at 33 MW [17]; applying that average slope (about 1.4 points per MW) as an indication only, the load difference could account for roughly 1.6–2.0 of the 9–10 points. The fuel gas flow fell by 11–14% while the load rose (Table 1), consistent in direction with the higher efficiency, but larger than the inlet pressure loss alone would suggest.

3.5. Causes of Filter Replacement: Fishbone and FMEA

Figure 2 shows the fishbone diagram. In the *Man* category, filter condition was monitored mainly by visual inspection, abnormal pressure drop could be recognised late, and installation errors and an uneven understanding of the actual filter condition were mentioned. In *Method*, replacement followed a fixed time interval and was not yet fully based on differential pressure, and the inspection procedure did not prevent late replacement. In *Machine*, dust and contaminants accumulated on the filter, and housing-seal leakage, differential-pressure sensor inaccuracy and clogging of the drain were possible additional contributors. In *Material*, filter quality governs the service life, and the media degrades with long use and with humidity or contamination. In *Environment*, the air around the plant carries high dust and particle loads; a dirty working environment, weather and humidity accelerate clogging and raise the replacement frequency. In *Measurement*, pressure-drop monitoring was not always the basis for replacement, a decline in filter performance could be detected late, and condition trending was not fully exploited.

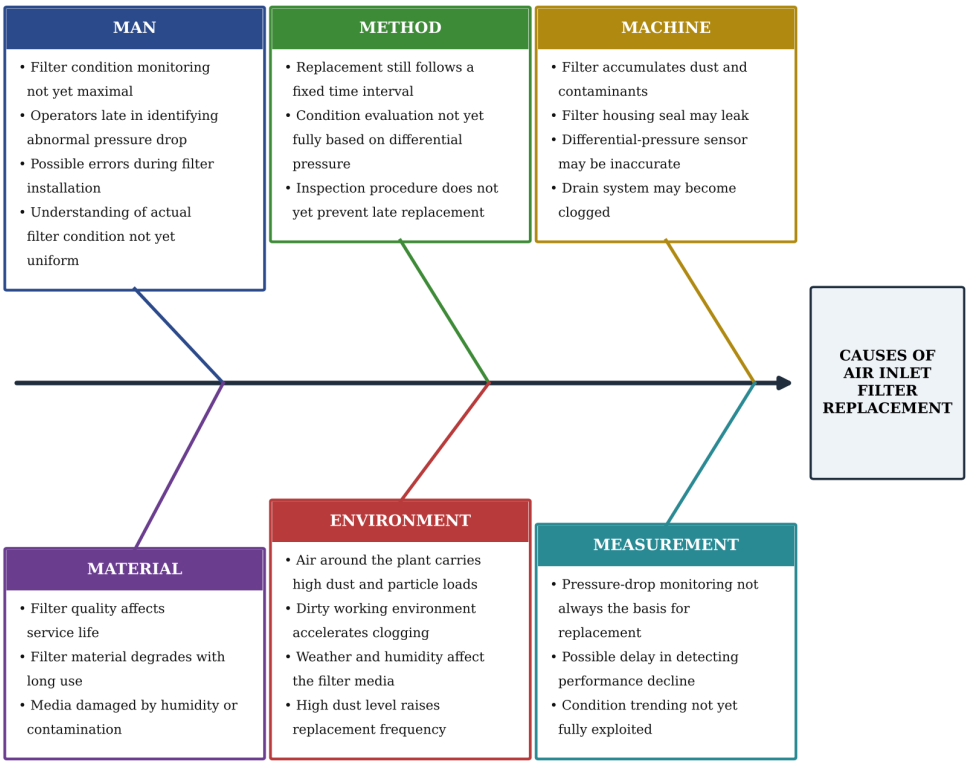


Figure 2. Fishbone (6M) diagram of the causes of air inlet filter replacement at GT1A.

Table 4 ranks the categories by RPN (Equation (13)). Environment has the highest priority (RPN = 126), followed by Material (80), Machine (64), Method (60), Measurement (45) and Man (36). The scores were assigned by the authors from interviews and observation, so they are subjective, and no dust concentration was measured at the site. The dominance of the environmental factor is therefore a qualitative finding.

Table 4. FMEA of the dominant failure mode in each fishbone category.

Rank	Category	Dominant failure mode and cause	*S*	*O*	*D*	RPN
1	Environment	Filter clogged by dust and contaminants; dusty surroundings, long cleaning interval	6	7	3	126
2	Material	Degraded filter media; service life, high humidity, material quality	5	4	4	80

Rank	Category	Dominant failure mode and cause	*S*	*O*	*D*	RPN
3	Machine	Leaking housing or seal; worn seal, imprecise installation, housing corrosion	4	4	4	64
4	Method	Replacement not matched to actual condition; interval-based, visual inspection	5	4	3	60
5	Measurement	Inaccurate DP sensor; irregular calibration, sensor contaminated by dust	5	3	3	45
6	Man	Lack of inspection thoroughness; limited experience, visual identification	4	3	3	36

3.6. Filter Service Life and Replacement Criterion

The filter was installed on 1 November 2022 and replaced on 19 November 2025, giving $T = 3.05$ years (Equation (11)) and $H = 3.05 \times 4{,}032 \approx 12{,}297$ h (Equation (12)). Over this period the filter differential pressure rose from 45 to 82 mmH_2O (441 to 804 Pa, +82%). The final value exceeds the final pressure drop of 600 Pa (≈61 mmH_2O) given in the specification of the air inlet filter. A condition-based criterion, in which replacement is triggered when ΔP_f approaches 61 mmH_2O instead of after a fixed 3 years or 12,300 h, is consistent with guidelines that base filter changeout on pressure drop and operating conditions [2]; Köse and Yılmazoğlu [10] found for a GT13E2 unit that replacement every 2,500 operating hours or at $\Delta p = 5$ mbar (≈51 mmH_2O) was the cost-optimal option, a threshold of the same order as the specified limit used here. If the pressure drop rose monotonically, such a criterion would have prompted replacement before 82 mmH_2O was reached. It is based on one replacement cycle and should be validated with continuous ΔP trending.

3.7. Limitations and Outlook

The conclusions are subject to the following limitations: (i) only two days with one reading per snapshot were compared, without uncertainty analysis, and November and January differ in season; (ii) the compressor wash carried out between the datasets confounds the effect of the filter replacement, so the two cannot be separated (Section 3.1); (iii) T_3 and the logged P_1 are DCS readings whose measurement uncertainty is not known; (iv) constant-property and no-pressure-loss assumptions affect absolute values; and (v) the efficiencies are temperature-based, because the air mass flow was not measured. Future work should include continuous ΔP and particulate measurements, compressor-wash records, a fuel-based efficiency using $\dot{m}_f$ and the lower heating value, uncertainty propagation, and several replacement cycles.

4. Conclusions

This study evaluated the effect of air inlet filter replacement on the GT1A gas turbine of Unit 1A of Bekasi Power Combined Cycle Power Plant. The main conclusions are:

1. After replacement, filter differential pressure fell from 76–82 to 45–46 mmH_2O (about 0.3 kPa), while compressor efficiency rose from 78.85–81.76% to 88.71–90.88%, combustion-chamber efficiency from 90.36–92.07% to 95.05–96.20%, turbine efficiency from 74.87–76.31% to 80.02–81.45% and thermal efficiency from 18.23–21.58% to 27.92–30.82%.
2. The direction and approximate size of the efficiency changes are robust to hot-gas properties (turbine about +5 points, thermal +8 to +10 points), but the 0.3 kPa pressure-loss reduction explains only a small part of them; a compressor wash performed in the same period is a major concurrent factor, so the effect of the filter replacement alone cannot be isolated.
3. Fishbone and FMEA analyses identified environmental factors, mainly airborne dust (RPN = 126), as the dominant cause of filter deterioration.

4. The filter served 3.05 years (about 12,300 h) and reached 82 mmH_2O, above the specified final limit of about 61 mmH_2O; a condition-based replacement criterion using ΔP_f is recommended.

Author Contributions: Conceptualization, G.F.A. and A.E.; methodology, G.F.A. and A.E.; formal analysis, G.F.A.; investigation, G.F.A.; data curation, G.F.A.; writing—original draft preparation, G.F.A.; writing—review and editing, A.E.; supervision, A.E. All authors have read and agreed to the published version of the manuscript.

Funding: This research received no external funding.

Acknowledgments: The authors would like to express their sincere gratitude to Bekasi Power Combined Cycle Power Plant for providing operational data and technical support during this research. The authors also thank the Department of Mechanical Engineering, Politeknik Negeri Jakarta, for academic guidance and support throughout the completion of this study.

Conflicts of Interest: The authors declare no conflict of interest.

Appendix A. Sample Calculation

Snapshot 11 November 2025, 12:00: $T_1 = 304.35$ K, $P_1 = 110$ kPa, $T_2 = 646.05$ K, $P_2 = 1012$ kPa, $T_3 = 1323.15$ K, $T_4 = 858.00$ K. Equation (1): $T_{2s} = 304.35\ (1012/110)^{0.2857} = 573.77$ K. Equation (2): $\eta_c = (573.77 - 304.35)/(646.05 - 304.35) = 78.85\%$. Equation (3): $\eta_{cc} = (1323.15 - 646.05)/(1323.15 - 573.77) = 90.36\%$. Equation (4): $T_{4s} = 1323.15\ (110/1012)^{0.2857} = 701.84$ K. Equation (5): $\eta_t = (1323.15 - 858.00)/(1323.15 - 701.84) = 74.87\%$. Equation (10): $\eta_{th} = (465.15 - 341.70)/677.10 = 18.23\%$. Hot-gas case: $T_{4s} = 1323.15\ (110/1012)^{0.25} = 759.7$ K, $\eta_t = 82.56\%$, $\eta_{th} = 21.91\%$.

References

1. Saravanamuttoo, H.I.H.; Rogers, G.F.C.; Cohen, H.; Straznicky, P.V.; Nix, A.C. *Gas Turbine Theory*, 7th ed.; Pearson Education: Harlow, UK, 2017.
2. Wilcox, M.; Baldwin, R.; Garcia-Hernandez, A.; Brun, K. *Guidelines for Gas Turbine Inlet Air Filtration Systems*; Gas Machinery Research Council, Southwest Research Institute: 2010.
3. Kurz, R.; Brun, K. Degradation in gas turbine systems. *J. Eng. Gas Turbines Power* **2001**, *123*, 70–77. https://doi.org/10.1115/1.1340629.
4. Meher-Homji, C.B.; Bromley, A. Gas turbine axial compressor fouling and washing. In Proceedings of the 33rd Turbomachinery Symposium, Houston, TX, USA; Texas A&M University: College Station, TX, USA, 2004; pp. 163–192.
5. Meher-Homji, C.B.; Chaker, M.; Motiwala, A.F. Gas turbine performance deterioration. In Proceedings of the 30th Turbomachinery Symposium, Houston, TX, USA; Texas A&M University: College Station, TX, USA, 2001; pp. 139–175.
6. Jin, Y.; et al. A novel integrated modeling approach for filter diagnosis in gas turbine air intake system. *Proc. Inst. Mech. Eng. Part A J. Power Energy* **2022**, *236*, 435–449. https://doi.org/10.1177/09576509211044392.
7. Simanjuntak, C.B.; Putra, I.Z.; Toar, H.; Aryeni, I. Analisis pengaruh penggantian air inlet filter terhadap kerja kompresor di PT. Energi Listrik Batam. *J. Rekayasa Energi* **2024**, *3*(1). https://doi.org/10.31884/jre.v3i1.53.
8. Purwanto, D. Analysis of the effect of inlet compressor temperature on the thermal efficiency of PLTG Unit 3.2 in Grati. *J. Mech. Des. Test.* **2024**, *6*, 101–114. https://doi.org/10.22146/jmdt.102262.
9. Effiom, S.O.; et al. Experimental study on the optimal performance of gas turbine (GT) inlet air filtration system for offshore application. *J. Eng. Appl. Sci.* **2023**, *70*. https://doi.org/10.1186/s44147-023-00303-8.
10. Köse, O.Ö.; Yılmazoğlu, M.Z. Gaz türbini periyodik bakımlarının sistem performansına etkilerinin incelenmesi [Investigation of the effects of gas turbine periodic maintenance on system performance]. *Mühendis ve Makina* **2025**, 718, 129–172. https://doi.org/10.46399/muhendismakina.1564458.

11. Liliana, L. A new model of Ishikawa diagram for quality assessment. *IOP Conf. Ser. Mater. Sci. Eng.* **2016**, *161*, 012099. https://doi.org/10.1088/1757-899X/161/1/012099.
12. Kumah, A.; et al. Cause-and-effect (fishbone) diagram: A tool for generating and organizing quality improvement ideas. *Glob. J. Qual. Saf. Healthc.* **2024**, *7*, 85–87. https://doi.org/10.36401/JQSH-23-42.
13. Stamatis, D.H. *Failure Mode and Effect Analysis: FMEA from Theory to Execution*, 2nd ed.; ASQ Quality Press: Milwaukee, WI, USA, 2003.
14. Moran, M.J.; Shapiro, H.N.; Boettner, D.D.; Bailey, M.B. *Fundamentals of Engineering Thermodynamics*; John Wiley & Sons: Hoboken, NJ, USA, 2018.
15. Çengel, Y.A.; Boles, M.A.; Kanoğlu, M. *Thermodynamics: An Engineering Approach*; McGraw-Hill Education: New York, NY, USA, 2019.
16. ISO 29461-1:2021. *Air Intake Filter Systems for Rotary Machinery—Test Methods—Part 1: Static Filter Elements*; International Organization for Standardization: Geneva, Switzerland, 2021.
17. Yohana, E.; Herriza, R.M. Analisis efisiensi siklus combine cycle power plant (CCPP) gas turbine generator terhadap beban operasi PT Krakatau Daya Listrik. *ROTASI* **2016**, *28*(1).